AD-A137 750 SPECTROSCOPIC STUDIES OF THE PRODUCTS OF THE REACTIONS OF EXCITED NOBLE-G..(U) PITTSBURGH UNIV PA DEPT OF CHEMISTRY M F GOLDE 29 JUN 83 PR81-00615 1/1

UNCLASSIFIED AFOSR-TR-84-0064 AFOSR-79-0089 F/G 7/4 NL

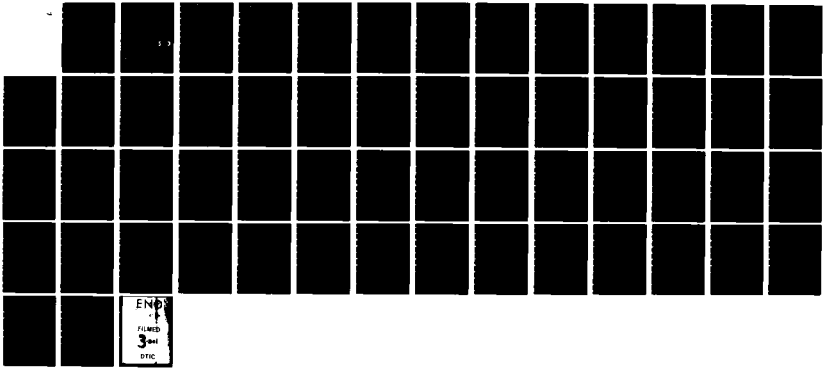

END

FILMED

3-84

DTIC

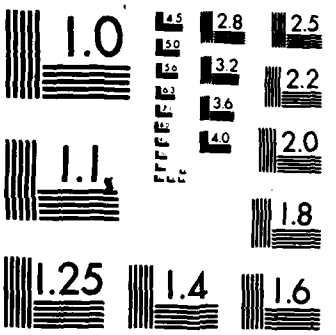

(12)

SECURITY CLASSIFICATION OF THIS PAGE (When Data Entered)

REPORT DOCUMENTATION PAGE

READ INSTRUCTIONS BEFORE COMPLETING FORM

1. REPORT NUMBER: AFOSR-TR- 84-0064
2. GOVT ACCESSION NO.: AD-A137750
3. RECIPIENT'S CATALOG NUMBER:

4. TITLE (and Subtitle): Spectroscopic Studies of the Products of the Reactions of Excited Noble-Gas Atoms

5. TYPE OF REPORT & PERIOD COVERED: Final Scientific Report 3/15/79 - 5/14/83

6. PERFORMING ORG. REPORT NUMBER: PR81-00615

7. AUTHOR(s): Michael F. Golde

8. CONTRACT OR GRANT NUMBER(s): AFOSR-79-0089

9. PERFORMING ORGANIZATION NAME AND ADDRESS:
University of Pittsburgh
Department of Chemistry
Pittsburgh, PA 15260

10. PROGRAM ELEMENT, PROJECT, TASK AREA & WORK UNIT NUMBERS: 2303/B1 61102F

11. CONTROLLING OFFICE NAME AND ADDRESS:
Air Force Office of Scientific Research/NC
Building 410, Bolling AFB, DC 20332

12. REPORT DATE: 6/29/83

13. NUMBER OF PAGES: 55

14. MONITORING AGENCY NAME & ADDRESS (if different from Controlling Office):

15. SECURITY CLASS. (of this report): Unclassified

15a. DECLASSIFICATION/DOWNGRADING SCHEDULE:

16. DISTRIBUTION STATEMENT (of this Report)

Approved for public release; distribution unlimited

17. DISTRIBUTION STATEMENT (of the abstract entered in Block 20, if different from Report)

---

18. SUPPLEMENTARY NOTES

19. KEY WORDS (Continue on reverse side if necessary and identify by block number)

Energy transfer, electronic-to-electronic; electronically excited noble gas atoms; resonance fluorescence; chemiionization.

20. ABSTRACT (Continue on reverse side if necessary and identify by block number)

The products of the very rapid reactions of electronically-excited Ar, Kr and Xe atoms with several oxygen-, hydrogen- and halogen-containing compounds have been investigated using the saturation ion-current technique and emission and atomic resonance fluorescence spectroscopy in discharge-

DD FORM 1 JAN 73 1473 EDITION OF 1 NOV 65 IS OBSOLETE

SECURITY CLASSIFICATION OF THIS PAGE (When Data Entered)

flow systems. New insight has been obtained into the mechanisms of the channels leading to chemiionization and noble-gas halide formation. Energy transfer leading to molecular dissociation is the major and often the dominant channel, with one or more atoms being eliminated in strong preference to elimination of molecular or electronically-excited fragments.

For the excited noble gas atoms, the high quenching efficiency and dominance of dissociation and ionization channels are associated with the availability of accessible acceptor states of the quenching molecule, as revealed by its absorption spectrum. It is proposed that these efficient reactions occur by energy transfer at relatively long range with no major prior distortion of the quenching molecule.

It is expected that this model should be directly applicable to the reactions of certain other excited species, which exhibit a similar correlation of quenching rate constants with the availability of acceptor states at the appropriate energy.

A. Introduction

Although many total quenching rate constants have been measured for electronically-excited atoms and small molecules,[1-3] much less is known about the nature of the reaction products.[2-7] The principal objective of this project was detection for the first time of the products of 'dark' reactions of metastable Ar, Kr, and Xe ($A^*{}^3P_{0,2}$) atoms with molecules, in which the product fragments are in their ground electronic states. The technique used, atomic resonance fluorescence detection of hydrogen, oxygen and chlorine atoms in a discharge-flow system, revealed a rich assortment of dissociation channels resulting from the energy transfer.

Simultaneous measurements of light emission intensity, resonance fluorescence intensity and ion production rates were made to provide the first direct and quantitative investigation of competition between allowed reaction channels for these species. These include:

Penning Ionization: $A^* + BC \rightarrow A + BC^+ + e^-$, (1)

and other related channels, such as associative and dissociative ionization and ion-pair formation;

Non-dissociative energy transfer: $A^* + BC \rightarrow A + BC^*$ (2)

Dissociation: $A^* + BC \rightarrow A + B + C$ (3)

Dissociative excitation: $A^* + BC \rightarrow A + B^* + C$ (4)

and atom-transfer chemiluminescent reaction (noble gas halide excimer formation): $A^* + RX \rightarrow AX^* + R$. (5)

In general, B, C and R are polyatomic fragments and X is a halogen atom. All 5 categories were observed, with dissociation clearly the major channel and dissociative excitation surprisingly unimportant for the reactions studied.

It was hoped that the results could be interpreted in terms of the primary interaction between the excited atom and the collision partner. Considerable progress towards this goal was achieved and a correlation obtained, relating the overall quenching rate constant for a given collision pair to the observed products and to properties of the reagent molecule. In addition, many comparisons between the observed channels and the known vacuum UV photochemistry of the reagent molecules were possible.

As a minor objective, making use of the discharge-flow technique, it was proposed to employ secondary reactions to yield information on the internal state distribution of certain product species. This was not successful in general, but the distributions of O atoms among the ^3P, ^1D and ^1S states, resulting from the reactions of Ar* and Xe* with O_2, were determined by this technique.

In the course of the project, a major extension of the technique allowed the twin metastable states, $^3P_0$ and $^3P_2$, of Ar to be separated, and chemiionization and channels leading to light emission were studied for state-selected Ar metastables.

Section B reviews the experimental techniques, with emphasis on novel methods developed as part of the project. Section C includes the principal results and section D presents their interpretation, especially in terms of the stated objectives and their possible impact on related areas of chemical kinetics and energy transfer. Relevant properties of the excited noble gases are listed in Table 1 and rate constants[1] for their reactions in Table 2. All the major findings of this project have been included in this report; however, many details of the experimental set-up, procedure and precautions and of the analysis, which have been described in the annual reports (1980-82) or in publications,[8-13] have been omitted.

B. Experimental Techniques.

The project involved the use of two discharge-flow systems, one for the resonance fluorescence measurements, the other for saturation ion-current measurements (see Figs 1,2). Both systems have been described in the annual reports and publications[10,11] and only the most important features are discussed here. In both systems, the reaction occurs by diffusion of a small flow of reagent gas into the bulk gas flow (mainly Ar at a pressure of 1 - 5 Torr), which contains the metastable atoms ($Ar(^3P_{2,0})$), $Kr(^3P_2)$or $Xe(^3P_2)$ at concentrations of about 10^{10} cm^{-3}) and which has a typical linear flow velocity of 50m s^{-1}. Because of the large rate constants of most of the reactions studied, the reaction is complete within 1 to 2 cm. Emission (110 - 800 nm) from this region is monitored directly via vacuum monochromators and photomultipliers.

B1. Resonance Fluorescence

In the resonance fluorescence system,[10] the reagent inlet assembly is made movable by means of O-ring seals and flexible connections to the rest of the vacuum system. Resonance fluorescence measurements are made 5 cm downstream of the reaction zone, allowing almost complete discrimination against emission from the reaction. This is important, for instance, in the reaction of Ar* with Cl_2, which produces extremely intense atomic emission at the wavelength used for resonance fluorescence.

Many designs for the lamp source for resonance fluorescence are available in the literature: in ours, the microwave cavity (conventional Evenson design) extended to within 1 cm of the MgF_2 window separating the lamp from the reaction vessel. By mounting the window in a teflon, rather than a metal, holder, the plasma was found to extend up to the window, yielding relatively intense, but

only moderately self-reversed atomic lines. Simple cylindrical blackened baffles, also of teflon,sufficed to reduce the scattered light to an acceptable level. For O- and H-atom detection, resonance fluorescence signals were typically 20 count s^{-1}, with a scattered light level of 3 s^{-1}; for Cl-atom detection at 134.7 nm, signals were larger and the scattered light less than 1 s^{-1}. The scattered light signal, measured with the discharge source of metastable atoms switched off, includes any resonance fluorescence of atoms produced by direct photodissociation of the reagent molecule. No such contribution was detected for any of the reagents studied.

All resonance fluorescence measurements were basically relative, the signal from the reaction A* + Q of interest being compared to that from a reference reaction of the same metastable. Considerable care was taken in establishing the absolute atom yield per reactive event (ie the quantum efficiency for conversion of A* atoms into atomic O, H or Cl product) for the reference reaction, as these were the source of all our absolute atomic yields; this involved searches for all possible competing channels, cross-checks of the H, O and Cl yields where possible, for instance via the reactions with HCl, and the use of reactions, whose product channels have been determined by other means, such as Ar* + Cl_2 and Ar* + N_2O. Excellent consistency was found among the results, so that the uncertainty in the atom yields due to such systematic errors is considerably less than 5%. The reference reactions used on a daily basis were (f = branching fraction):

$$A^* + O_2 \rightarrow A + O + O \quad , f = 1.00 \tag{6}$$

$$A^* + H_2 \rightarrow A + H + H \quad , f = 1.00 \tag{7}$$

$$A^* + CF_3Cl \rightarrow A + CF_3 + Cl \quad , \tag{8}$$

for which f = 0.95 ± 0.03 for Ar* and f = 0.97 ± 0.02 for Kr* and Xe*.

To test for absorption of the resonance radiation by the reagent molecules, an Al surface mounted on a movable rod was inserted into the observation region to reflect radiation from the lamp into the monochromator. The detected intensity, as a function of reagent concentration in the reaction vessel, was analyzed by the Beer-Lambert law to yield an effective absorption cross-section, $\sigma.\ell$, used where necessary in correction of the resonance fluorescence data.

B2. Saturation Ion-Current Measurements

For reactions of Ar*, total yields of chemiionization were measured by the saturation ion-current technique,[11] in which all the positive ions were swept by an applied electric field to a grounded grid and the grid current measured as a function of applied field. While this yields the absolute ion flux directly and relative ion yields from the reactions (using Ar* + NO or CF_2Br_2 as reference reactions), the absolute flux of Ar* metastables is also required for the determination of chemiionization branching fractions. The technique used, involving measurements of emission intensities from the well-characterized reactions of He* and Ar* with N_2 and the ion-current from He* + N_2, has been described fully. This calibration technique is inferior to that used for the resonance fluorescence measurements. Firstly, the relevant branching fractions in these calibration reactions have uncertainties of about 20%. Secondly, because of the much greater mobility of charged particles in He than in Ar, a less satisfactory saturation ion-current was obtained in the He* + N_2 reaction, it being very difficult to select conditions which entirely eliminated the twin evils of secondary ionization and ion-electron recombination. As a result, the absolute chemiionization branching fractions were estimated to have an uncertainty of ± 35%. Subsequent experiments, in which ion-current and resonance fluorescence data provided complementary information on the channels for a given

reaction, showed no instances of inconsistencies in the data and suggested that the true uncertainty in the ion branching fractions is no larger than +20%, -15%.

Ion-electron recombination was also found to occur in the reactions of Ar* with specific reagents. It was characterized by the effect of very small additions of SF_6 ($1 - 6 \times 10^{12}$ cm^{-3}) with the reagent on the reaction products, in causing up to a 2-fold increase in the saturation ion current and decreases of up to 30% in the resonance fluorescence signals. Only a small group of reactions, those of Ar* with NH_3, CH_3OH, CH_2O, C_2H_5OH, CH_3OCH_3, OCS, CH_3Cl, CH_2Cl_2 and CH_3Br, showed these effects. The investigation of this effect has been described;[13] it was concluded that SF_6 eliminates the ion-electron recombination through highly-efficient scavenging of the electrons (ion-ion recombination is significantly slower than ion-electron recombination) and that the data obtained in the presence of SF_6 are valid.

Several additional checks of the validity of the saturation ion-current technique were possible. For instance, addition of reagents such as N_2 or O_2, which cannot be ionized by Ar*, gave residual ion currents of about 10^{-10} to 10^{-9}A, compared to the ion current of about 6μA from Ar* + NO. Similarly, if the Ar* metastables were destroyed by illumination of the flow tube with Ar resonance radiation, the ion-current dropped appropriately. Finally, negative-ion or electron currents measured at the positively-biased electrode closely matched (apart from sign) the measured grid current.

Towards the end of the project, experiments commenced on chemiionization by Ne* metastable atoms. Although saturation ion-currents were obtained and the current was lowered more than 10-fold by destroying the metastables using a Ne lamp, no true background signal can be measured, as all reagents, which react at an appreciable rate with Ne*, are ionized to a significant extent. Because of this and the small number of experiments carried out as yet, the results presented in the next section must be considered as preliminary.

B3. Reactions of $Ar(^3P_0)$ and $Ar(^3P_2)$.

Measurements by several workers have shown that, in a flow system, the Kr and Xe metastables are formed principally in the $^3P_2$ state, but that a small fraction, less than 20%, of the Ar metastables are in the $^3P_0$ state. Our discovery[8] that Kr quenches $Ar(^3P_0)$ at least 20 times more slowly than it quenches $Ar(^3P_2)$ provided the basis of a method to study the former species. Briefly, a small flow of Kr was added to the flow upstream of the main reagent inlet and preferentially removed the $^3P_2$ metastable. The products of the reaction of $Ar(^3P_0)$ with the reagent of interest were then studied in the normal way. In many experiments, the relevant ion current or emission intensity was monitored as a function of Kr flow rate. No resonance fluorescence measurements were attempted, principally because of possible interference from the products of the reaction of the Kr* metastables, formed from the reaction of $Ar(^3P_2)$ with Kr.

The primary information from these measurements is α_0, the fraction of the observed signal in the absence of Kr, which is due to the reaction of $Ar(^3P_0)$. In terms of branching fractions, f_0 and f_2, for the occurrence of this channel in the reactions of respectively $Ar(^3P_0)$ and $Ar(^3P_2)$,

$$\alpha_0 = \frac{f_0[Ar^3P_0]}{f_0[Ar^3P_0] + f_2[Ar^3P_2]} \qquad (i)$$

In most cases, f_2 is close to the branching fraction obtained in the usual (state non-selected) experiments. Extraction of values of f_0 requires knowledge of the concentration ratio, $[Ar^3P_0]/[Ar^3P_2]$. This has been estimated from reactions in which all the expected reaction channels, i, can be observed, so that $\sum_i f_{0i} = \sum_i f_{2i} = 1$. The reactions used were:

$$Ar^* + Cl_2 \rightarrow ArCl^* + Cl \quad (9)$$

$$\rightarrow Ar + Cl^* + Cl \quad (10)$$

$$\rightarrow Ar + Cl_2^* \quad (11)$$

$$Ar^* + Br_2 \rightarrow Ar + Br^* + Br, \quad (12)$$

in which all the excited product states emit strongly.

C. Results.

C1. Saturation ion-current measurements

The dependence of the measured ion current on the applied electrode potential for the reactions of Ar* with C_2H_5OH and CH_3OCH_3 is shown in Fig. 3. The effect of the presence of SF_6 is shown clearly, as are the excellent saturation ion-currents obtained, in the presence of SF_6, over a wide range of voltage. For those reagents, which showed an SF_6 effect, saturation ion-currents obtained in the absence and presence of SF_6 are listed in Table 3 and the Ar* chemiionization branching fractions, including, where relevant, data obtained in the presence of SF_6, appear in Table 4. As discussed in the previous section, these data refer to ionization by a mixture of $Ar(^3P_2)$ and $Ar(^3P_0)$, the former being in approximately 10-fold excess. Using Kr to remove the $Ar(^3P_2)$ metastable (see Fig 4 for typical data), values of α_0 were measured and the derived branching fractions, f_0 and f_2, for chemiionization by $Ar(^3P_0)$ and $Ar(^3P_2)$ respectively are listed in Table 5.

Some significant features of these results are summarized below.

a) Very little ionization is observed for reagents with ionization potentials significantly greater than the energies of the $Ar(^3P_{0,2})$ metastables (see Table 1), but for which ion-pair formation is exothermic, e.g.

$$Ar^* + HCl \rightarrow Ar + HCl^+ + e^-, \quad \Delta H = +1.2eV \qquad (13)$$

$$\rightarrow ArH^+ + Cl^- , \quad \Delta H \sim -0.8eV \qquad (14)$$

These results and analogous tests with Kr* metastables suggest that ion-pair formation is not generally important and that Penning and associative ionization are the major ionization channels involved (dissociative ionization is endothermic for almost all the reactions studied).

b) Branching fractions for chemiionization are considerably below unity in all cases. This contrasts with accepted behavior for the reactions of He* and Ne*,[7] although previous data for their reactions are not sufficiently precise to rule out significant contributions from channels other than ionization.

c) Three reagents, Br_2, Cl_2 and NO_2, show anomalously small ionization branching fractions. It is noteworthy that these reagents have unusually large electron affinities.

d) f_0 and f_2 are in general similar for a given reagent. However, the differences in Table 5 are outside experimental error limits. For the reagents with ionization potentials close to 11.5eV, these differences are very large, indicating that chemiionization increases sharply with energy above threshold.

Saturation ion-currents obtained in several reactions of Ne* (in the presence of SF_6) appear in Table 6. Relative ion yields are also given; it is expected that these correspond approximately to branching fractions. The main surprise was the large range in the saturation ion-currents obtained, clearly indicating that Ne*, like Ar*, induces channels other than ionization with appreciable efficiency. Preliminary observations of other reaction channels support this finding.

C2. Emission measurements

Many previous studies of light emission from electronically-excited products of noble-gas metastable reactions have been reported (see for example refs. 7, 14-21). In particular, Setser and coworkers[22-25] have obtained many branching fractions for noble-gas halide excimer formation (reaction (5)) and a smaller number of branching fractions for nondissociative energy transfer, equ. (2), and dissociative excitation, equ. (4). Therefore, our studies have been limited to a few specific reactions and to the separate reactions of $Ar(^3P_2)$ and $Ar(^3P_0)$.

Most of the emitting states studied in this project have sufficiently short radiative lifetimes for the entire reaction flame to be confined within the field of view of the monochromator. Under these conditions, the emission intensity was approximately independent of reagent flow rate and branching fractions were obtained by comparing the integrated emission intensity (including spectral response corrections) with that from reference reactions. For the UV and visible, the reference reactions were:

$$Ar^* + N_2 \rightarrow Ar + N_2(C^3\Pi_u), \quad f = 0.8 \pm 0.2 \text{ (ref. 10)} \quad (15)$$

$$Kr^* + Cl_2 \rightarrow KrCl^* + Cl, \quad f \sim 1.0 \quad (16)$$

For the vacuum UV, the reference reaction was

$$Ar^* + Br_2 \rightarrow Ar + Br^*(5\,^4P_J,\ ^2P_J) + Br, \quad f \sim 1.0 \quad (17)$$

For species with larger radiative lifetimes, such as $CO(a^3\Pi)$(7ms), $O(^1S)$(0.8s) and $O_2(b^1\Sigma_g^+)$(12s), the fraction of excited species emitting within the field of view was estimated in order to determine branching fractions for emission. Relevant branching fractions, including our results and those of other workers, are listed in Table 7. Emission from reactions mentioned elsewhere in this report, but not included in this table, was generally weak, although it should be stressed that such reactions remain a valuable source of emission spectra of little-studied radicals and ions. The present project revealed several weak emission features of possible interest. Among these were strikingly-similar visible spectra from the reactions of $Ar^* + CF_3Cl$, $Ar^* + CF_3H$ and $Kr^* + CF_3Br$, which have been very recently ascribed[21] to transitions of CF_3.

An unexpected finding was that of intense emission from $Xe(^3P_1)$, resulting from the reactions of Xe^* with CF_4 and CF_3H.

$$Xe(^3P_2) + CF_3H(CF_4) \rightarrow Xe(^3P_1) + CF_3H(CF_4) - 0.25eV. \quad (18)$$

No precise branching fraction has been measured but approximately every collision with sufficient energy to overcome the considerable endothermicity of this

process leads to $Xe(^3P_1)$ formation. These reactions have unusually small rate constants (see Table 2); as yet, no other reaction has been found to yield comparably strong $Xe(^3P_1)$ emission.

Emission of ArCl* and $Br^*(5^{2,4}P_J)$ from the separate reactions of $Ar(^3P_2)$ and $Ar(^3P_0)$ with several compounds was studied in considerable detail. Remarkable differences in the spectra were found, as illustrated in Fig 5, for $Ar^3P_{0,2}$ + CCl_4, and in Table 8, for reaction with several Br-containing reagents. $Ar(^3P_0)$ appears to induce a new transition of ArCl, ascribed to the (D-X) system, and $Ar(^3P_2)$ is anomalously ineffective at populating the $^{2,4}P_{1/2}$ levels of Br*. These findings have been discussed already.[9] Values of the parameter α_0 were determined for several of these reactions and these and estimates of f_2 and f_0 for total emission are listed in Table 9. In contrast to the high values of α_0 found typically for chemiionization, f_0 is generally less than f_2 for emission in the reactions studied, with a remarkably small value of f_0/f_2 for CH_2Br_2.

These studies, especially those using Cl_2 as the principal reagent, yielded relative rate constants, $k_0(Kr)/k_2(Kr)$, for the quenching of respectively $Ar(^3P_0)$ and $Ar(^3P_2)$ by Kr. Analogous measurements of k_0/k_2 were made for several other inefficient quenchers of Ar*. The ratios k_0/k_2 obtained for Kr, CO, H_2, D_2, CH_4 and CF_4 are, respectively: ~0.050, 8±1, 1.51±0.07, 1.56±0.07, 1.26±0.06, and 0.54±0.03.

C3. Resonance fluorescence measurements.

Each reaction was studied over a range of reagent concentration. All experiments included measurements of background emission (resonance lamp off, A* source on) and scattered light (resonance lamp on, A* source off) and the resonance fluorescence signals were corrected for these contributions. As shown in Fig 6 for Xe* + H_2, except at very small flowrates of reagent, the resonance

fluorescence signal is independent of concentration, corresponding to complete conversion of the metastable atoms to reaction products. The effect of SF_6 addition on atom yields is included in Table 3. Addition of comparable amounts of SF_6 had no effect on the atom yields from other reactions of Ar* nor on those from any reactions of Kr* and Xe* studied. The final atom yields are listed in Tables 10-12; the quoted uncertainties are the standard deviations of the data of each reaction. These were measured relative to the yields from the reference reagents, respectively O_2, H_2 and CF_3Cl in these tables, but should represent absolute yields of atoms per reactive event (ie quantum yields for conversion of the metastable noble gas atom into the product atoms). Table 10 contains results for small O-containing compounds. Table 11 includes H-atom yields, together with some O-atom yields, where relevant, from the same H-containing reagent. Table 12 presents Cl-atom yields for chloromethanes and a few related compounds. Relevant H yields are included; a few preliminary F-atom yields have been obtained, but are not included.

Several precautions had to be taken to ensure the validity of the tabulated results.

a) Absorption corrections. For several reagents, including N_2O, CH_4 and the chlorofluorocompounds, a small inverse dependence of resonance fluorescence signal on reagent concentration in the range (0.3 to 2) x 10^{14} cm^{-3} was seen, due to absorption of the O, H or Cl resonance radiation. All of these data were corrected,using the effective absorption coefficients, $\sigma.\ell$ (see section B):

$$I_{corr} = I_{meas} \cdot \exp(\sigma.\ell.[Q]) \qquad (ii)$$

Most corrections were below 10% and none greater than 20%, and the corrected data exhibited no significant flow dependence.

b) Electronic state of O and Cl. The resonance fluorescence technique was developed for detection of O atoms in the ^3P_J states (with an assumed Boltzmann

distribution among the J = 0, 1 and 2 spin-orbit components) and for detection of Cl atoms in the $^2P^o_{3/2}$ state. For oxygen atoms, formation in the ^1D or ^1S states was also exothermic in several reactions. Several species, including the buffer gas, Ar, quench $O(^1S)$ only slowly, so that this species would not be detected by resonance fluorescence. Formation of $O(^1S)$ was sought via the $O(^1S-^1D)$ emission at 557.7 nm; although it was observed in some reactions, the derived yields of $O(^1S)$ were extremely small in all cases. $O(^1D)$ is quenched by Ar efficiently to the $O(^3P)$ state, so that, under normal conditions, any $O(^1D)$ would be detected, following the relaxation, by the resonance fluorescence technique, yielding reliable <u>total</u> O-atom concentrations. Scavenging experiments, employed to gain additional information concerning the nascent O-atom state distribution, have been described.[10,12] For Kr* + SO_2, it was concluded that approximately 20% of the O atoms are formed in the $O(^1D)$ state; no evidence for $O(^1D)$ formation in Ar* + SO_2 was obtained. For Xe* + O_2, no significant yield of $O(^1D)$ was found, in sharp contrast to photodissociation of O_2 at the nearly equivalent wavelength of 147 nm. For Ar* + O_2, the data could be expressed in terms of the following branching fractions:

$$Ar^* + O_2 \rightarrow Ar + O(^3P) + O(^3P) \quad , \quad f = 0.46 \pm 0.18 \qquad (19)$$

$$\rightarrow Ar + O(^3P) + O(^1D) \quad , \quad f = 0.52 \pm 0.18 \qquad (20)$$

$$\rightarrow Ar + O(^3P) + O(^1S) \quad , \quad f = 0.02 \pm 0.01 \qquad (21)$$

For Cl atoms, formation in the excited spin-orbit state, $Cl(^2P^o_{1/2})$, is possible. This was tested via resonance fluorescence measurements at 135.2 nm, the $^2P_{1/2} - {}^2P^o_{1/2}$ transition. Evidence for $Cl(^2P^o_{1/2})$ formation was obtained only in the reactions of Ar*, Kr* and Xe* with HCl, and it was found that, by employing a high gas pressure of 3-4 Torr and a reduced pumping rate, the excited atoms could be collisionally relaxed to the $^2P^o_{3/2}$ state upstream of the observation region. These conditions were used to ensure reliable total Cl-atom yields.

c) Secondary reactions. Because of the extremely large rate constants of the primary reactions and the small concentration of product species, the only possible secondary reactions of importance (other than the ion-electron processes discussed already) are fast reactions of a reaction product with the parent reagent molecule. Unless the secondary process occurs fully at the collision rate, such processes would be detected by a dependence of fluorescence intensity on reagent concentration. Such behavior was found only for A* + NO and NO_2, due to the secondary processes:

$$N + NO \rightarrow N_2 + O \quad (22)$$

$$O + NO_2 \rightarrow NO + O_2 \quad (23)$$

These effects have been discussed elsewhere.[10]

The very fast reaction

$$C_2H + C_2H_2 \rightarrow C_4H_2 + H \quad (24)$$

prevented study of the reactions with C_2H_2. No evidence was found for secondary processes in any other reaction studied, in agreement with published rate constants for possible reactions.

To conclude this section, a few noteworthy features of the results in Tables 10-12 are presented.

(i) The atom yields show clearly the importance of the dissociation channel. As is clear from a comparison of these tables with Table 7, the dissociation channel generally involves formation of fragments in non-emitting states; ie the 'dark' channel is, indeed, the major channel in most of the reactions studied. Clearly, previous studies of light emission or ion production have not revealed the full picture of the chemistry of the excited noble gases.

(ii) The dissociation channels favor the rupture of terminal C-H or O-H bonds over that of central bonds. For instance, dissociation of CH_3OH to CH_3 + OH or of C_2H_6 to CH_3 + CH_3 are <u>not</u> major channels.

(iii) Where exothermic, elimination of more than one H or Cl atom is a major and, in some cases, the dominant channel. The reactions of Xe* with CH_2O and CF_2Cl_2 and of Ar* with $CFCl_3$ are particularly striking examples.

(iv) In general, the atom yields vary smoothly with metastable energy. The reactions with chlorofluorocompounds present exceptions in the low Cl yields from the reactions of Kr* with CF_2Cl_2, $CFCl_3$, $CF_2Cl{\cdot}CF_2Cl$ and CF_3CCl_3.

D. Discussion

Extensive new data concerning the reactions of excited noble gas atoms have been presented in the previous section. Although each reaction shows specific points of interest, this discussion is directed mainly at the major objective of this project: an interpretation of the results in terms of the primary interaction between the excited atom and the collision partner. The results are too fragmentary to elucidate such interactions completely; however, as will be described, most of the data appear to fit a single pattern.

There are few possibilities for comparing our data with those for other excited species, because of the dearth of information on products of reactions of high-energy excited species, including most Rydberg states of non-metallic and metallic atoms and most excited states of molecules. Thus, a crucial aspect of this study is its applicability to other metastable excited states and data and arguments will be presented to suggest its considerable use in this respect.

The results reveal that dissociation of the molecule is normally the major reaction channel. The primary channels which can lead to atom production include not only the 'dark' channels of interest but also dissociative excitation, dissociative or rearrangement ionization and noble gas halide excimer formation. The contributions of dissociative excitation and excimer formation can be assessed by the use of Table 7; for the molecules listed in Tables 10-12, these channels are dominant only for Ar* + N_2O and Ar*, Kr* and Xe* + Cl_2, and are of moderate importance only for Ar* + CO_2, NO_2, H_2O, CCl_4 and CH_2O and for Xe* (and probably Kr*) + CCl_4 and $CFCl_3$. Dissociative and rearrangement ionization are expected to be endothermic, except for dissociative ionization of CCl_4 and $CHCl_3$, which by analogy with photoionization[26], is expected to be the major channel for ionization by Ar*. Combining these data with the atom yields of

Tables 10-12, branching fractions for many dissociative channels can be determined to good precision and these appear in Table 13, which also includes the theoretical threshold energies for these channels.

D1. Quenching Mechanisms

The main part of this section is devoted to a discussion of the branching fractions in terms of the possible reaction mechanisms. Clearly, a complete description of the mechanism for a single reaction requires:

(i) a knowledge of all relevant potential surfaces for the system;

(ii) a knowledge of all interactions between these surfaces;

(iii) analysis of the dynamics of the system, e.g., the outcome of trajectories, commencing on the reactant surfaces.

Because such information is not available as yet (initial insight into item (i) has recently been obtained for the simplest prototype reaction systems), approximate models have been proposed. For the excited noble gases, A*, the most commonly cited are:[7,1,27]

a) quenching via a long-range dipole-dipole (or higher multipole) interaction, whereby the energy transfer induces excitation of the reagent molecule, Q, according to radiative selection rules and the quenching cross section depends on the transition dipole moments of the noble gas and reagent molecule.

b) Quenching via an attractive charge-transfer (CT) intermediate state, A^+Q^-. In the simplest form of this model, an electron-jump from A* to Q induces a transition from the entrance surface to the CT surface at a specific separation, r_c, of A and Q (dependent on the ionization potential of A* and the electron affinity of Q). The quenching cross-section is πr_c^2, as quenching is assumed to occur with unit probability once the electron-jump has occurred.

c) Quenching via a curve-crossing from a reactant surface directly to a product

surface (without the intermediacy of a CT state). This has generally been discussed in terms of a crossing at short range, where there may be very strong attraction or repulsion between the reagents: in this form, it would be appropriate to the small number of slow quenching reactions of the excited noble gases. However, it can also be applied to crossings occurring at longer range, which would be appropriate for efficient quenching agents: the rate of energy transfer is then given by the Fermi golden-rule expression.[28]

In principle, any or all of these models can apply: unless a long-lived complex is formed, it is expected that the mechanism which induces quenching at the longest range will be the most important for a given reaction.

Existing rate constant data are not wholly consistent with either of the first two models, but it is not clear whether minor refinements of the models would suffice to perfect the fit, or whether the observed approximate correlations with appropriate molecular properties are fortuitous. The present data give valuable additional information, especially as comparison with the photochemistry of the reagent molecules gives insight into the applicability of the dipole-dipole model and as noble-gas halide excimer formation is known to occur solely via a CT intermediate, thus giving more direct information on this channel. The analogy with 'harpooning' reactions[29] of ground state alkali atoms is also relevant.

The important results of this study are now reassessed in terms of these models. It is concluded that, except where very strong noble-gas halide emission is seen, quenching occurs mainly by the third mechanism, causing the energy to be transferred efficiently into high energy dissociative or ionized states of the reagent molecule.

D2. The Charge-Transfer Mechanism

The yields of noble-gas chloride excimers from the reactions with the chloromethanes and fluorochloromethanes (and with many other chlorine-containing reagents, RCl) are small. This result has been interpreted[23] as implying that, following an initial electron jump to yield the CT intermediate, A^+RCl^-, further curve-crossings occur, leading to A + RCl*, rather than to ACl*+R. However, several of the analogous total cross-sections for the reactions of (ground-state) alkali atoms with these reagents are also small, and considerably smaller than the total A*+RCl quenching cross-sections. This implies that the competing dissociation (and chemiionization) channels occur at longer-range, where the species are still too far apart for charge transfer to occur. It is concluded that, for reagents with small or negative electron affinities, CT is unlikely to provide the major mechanism for quenching of excited noble gas atoms; other longer-range effects will prevail.

Several additional comments should be made here. Firstly, our earlier data[11] on the reactions with the chloromethanes, CCl_nH_{4-n}, which showed that the chemiionization branching fraction, f_{ion}, decreased as n increased, proved misleading, as they were taken to suggest that CT, which is expected to increase in importance with n, accounted for most of the reaction not leading to chemiionization. The more recent ionization data for $Ar(^3P_0)$ (Table 5) showed a much smaller dependence of f_{ion} on n, suggesting that threshold energy effects were responsible for much of the $Ar(^3P_2)$ effect. Secondly, it should not be concluded that excimer formation is the only allowed reaction channel following an electron jump. The ionization branching fractions for Ar* + Cl_2, Br_2 and NO_2 (Table 4) are extremely small, and those for Ne* + Cl_2 and NO_2 (Table 6) are likewise smaller than other entries in this table, suggesting that, following the expected initial electron jump to give A^+Q^-, the 2-electron loss from Q^- to give

Q^+ is unfavorable compared to competing channels. Thus chemiionization from the CT surface is not efficient but it undoubtedly occurs to some extent, as confirmed by Penning ionization electron spectra for He* + NO_2 and SO_2.[30,31] However, the competing process for Ar* + NO_2 involves dissociation of the NO_2 (Table 10), so that an electron jump from A^+Q^- to A-Q* is an allowed and, in some cases, an important process. Thirdly, charge transfer may be important if no longer-range interactions exist. Thus, ab initio calculations on Na*(3^2P) + H_2, for instance, reveal an attractive reactant surface,[32] which has at least partial charge-transfer character in the region in which crossing to the product surface occurs.

D3. Comparison with vacuum-UV photochemistry. In assessing the possible mechanisms for energy transfer, it is of interest to compare the results with those of photochemistry of the same molecules, especially that using Ar(104.8, 106.7 nm), Kr (123.6 nm) and Xe (146.9 nm) radiation.[33] For slow quenchers, H_2, CO and N_2, there are sharp differences between photochemistry and the metastable-induced chemistry, which can be ascribed to spin conservation, favoring population of singlet and triplet excited states respectively. The same factor may be responsible for the virtual absence of O(^{1}S) among the products of Ar* + CO_2, in contrast to photolysis between 105 and 110 nm.

The most significant difference between energy transfer and photodissociation for the efficient quenchers is the importance of molecular elimination in the latter case. In particular, the most striking feature of the vacuum UV photochemistry of CH_4, C_2H_6, NH_3 and CH_2O is the elimination of H_2, which has branching fractions[34-38] between 0.10 and 0.85. The higher yields, especially from C_2H_6 and CH_2O, are incompatible with the high H-atom yields observed in the present study and indeed the data in Table 13 show H_2 elimination to be

consistently a minor channel at best. It has recently been argued[39] that photodissociation of CH_4 to $CH_2 + H_2$ should be expected to be favored over production of $CH_3 + H$, at threshold at least, on symmetry grounds and it may be that the lower symmetry induced by the noble gas atom is in part responsible for the differences. The possibility that the difference arises because the noble gas generally transfers its energy with low efficiency can be ruled out. The results for CH_2O and C_2H_6 show the metastables to induce high-energy channels more readily than the isoenergetic photons.

Because of the consistent differences between the products of energy transfer and photon excitation, it must be concluded that, in the former case, the molecules are not necessarily excited in accordance with radiative selection rules and thus that the long-range dipole-dipole mechanism is not dominant in the quenching of the $A(^3P_2, ^3P_0)$ excited noble gas atoms. This result should not be surprising, because of the metastability of these species, but the large quenching rate constants, comparable to those of resonance states, has obscured the issue and led previously to the suggestion that the metastable states pick up partial singlet character during the collision.

The remainder of this section of the discussion is focused on the third mechanism, involving curve-crossing, either at short or long range. The aim of the discussion is to present evidence that, for efficient quenchers, energy is transferred without extensive prior distortion of the reagent molecule.

D4. Dependence of Branching Fractions for Ionization and Dissociation on Metastable Energy.

On the assumption that the chemiionization branching fraction for Ne* + Ar is close to unity, comparison of Tables 4 and 6 shows that Ne* induces a somewhat higher chemiionization branching fraction than does Ar* for each

reagent studied. Taken with the results for the reactions of $Ar(^3P_0)$ with CH_nCl_{4-n} and HBr (Table 5), it appears that chemiionization switches on sharply close to threshold, but then increases in importance only slowly at higher excitation energies.

Dissociation channels generally show contrasting behavior, becoming important only several eV above threshold. Examples include:

(i) $Kr^* + H_2O \rightarrow Kr + H + H + O + 0.5eV$, $f = 0.11\pm0.05$ (25)

$Ar^* + H_2O \rightarrow Ar + H + H + O + 2.0eV$, $f = 0.46\pm0.05$ (26)

(ii) $Xe^* + CH_2O \rightarrow Xe + CH_2 + O + 0.6eV$, $f = 0.03\pm0.01$ (27)

$Ar^* + CH_2O \rightarrow Ar + CH_2 + O + 3.8eV$, $f = 0.21\pm0.03$ (28)

(iii) $Xe^* + CH_2O \rightarrow Xe + CO + 2H + 3.8eV$, $f = 0.94\pm0.04$ (29)

ie this channel is dominant, but highly exothermic.

(iv) $Xe^* + CF_3Cl \rightarrow Xe + CF_2Cl + F + 2.9eV$, $f \leq 0.03\pm0.02$ (30)

ie., although this is strongly exothermic, this channel cannot compete with the still more exothermic dissociation to $CF_3 + Cl$.

Two notable exceptions should be mentioned:

(v) $Ar^* + CO \rightarrow Ar + C + O + 0.4eV$, $f = 0.84\pm0.02$ (31)

but note that this is a relatively slow reaction.

(vi) $Xe^* + CF_2Cl_2 \rightarrow Xe + CF_2 + 2Cl + 2.6eV$, $f > 0.96^{+0.04}_{-0.08}$

D5. Reaction Channels for the "Slow" Quenchers

Reactions which have rate constants close to the collision number occur solely by one or more of the channels: chemiionization, dissociation (including dissociative excitation) and excimer formation. As discussed above, all these channels must be capable of occurring at medium-to-large separations of the reagents. A more surprising feature of the results was the finding of additional channels for reactions with rate constants significantly below the collision rate, but for which the dissociation channel remained open. These additional channels were: non-dissociative energy transfer:

$$Ar^* + N_2 \rightarrow Ar + N_2^*(C^3\Pi_u), \qquad f = 0.80\pm0.20 \tag{33}$$

$$Ar^* + CO \rightarrow Ar + CO^* \qquad f = 0.16\pm0.02 \tag{34}$$

$$Ar^* + H_2 \rightarrow Ar + H_2^*(a^3\Sigma_g^+) \qquad f = 0.05 \tag{35}$$

and the highly endothermic excitation of $Xe(^3P_2)$ to $Xe(^3P_1)$ by CF_4 and CF_3H (equ. (18)), for which the branching fractions are estimated to be ~0.01. These processes are, therefore, characteristic of shorter-range interactions of the species and a feature of these slower reactions is clearly the absence of an efficient long-range interaction leading to molecular dissociation.

The key to understanding this behavior appears to be provided by the absorption spectra of these molecules, which reveal the location of excited states, which may act as acceptor states in the energy transfer: none of these five molecules shows continuous absorption at photon energies similar to that of the relevant noble-gas metastable. In contrast, for all the efficient quenching processes which have dissociation as the dominant channel, the absorption spectra reveal that dissociative states of the molecule are accessible in the undistorted molecule.

The rate constant data for CF_4 and CF_3H are particularly striking. Their spectra show absorption thresholds of about 12.0eV and 10.1eV respectively. The rate constants, for reaction with Ar*(11.5eV), Kr*(9.9eV) and Xe*(8.3eV) are: for CF_4: 4×10^{-11}, 7×10^{-13} and 3×10^{-13} cm^3s^{-1}, and for CF_3H: 3.1×10^{-10}, 1.5×10^{-10} and 2×10^{-12} cm^3s^{-1} respectively. N_2, CO and H_2 show <u>banded</u> absorption and the density of states nearly resonant with the metastables is apparently too low for quenching to be very efficient; however, energy transfer to relevant excited states (actually triplet states are favored for H_2 and N_2) lead to the observed parent emission.

The slow onset of dissociation channels above threshold for efficient quenchers can be understood similarly. Note that dissociation of CF_4 and CF_3H

by Xe* is strongly exothermic, but is difficult to achieve as the relevant dissociating state must be strongly repulsive. It can only be accessed either by considerable distortion of the molecule or by excitation far above the dissociation limit. Thus, there is a large energy barrier to dissociation. Almost all the molecules studied show, similarly, absorption spectra which commence at much higher energies than their first dissociation energies. The case of Xe* + CF_3Cl, equ (30), is particularly interesting: the excited state populated dissociates to CF_3 + Cl, but an additional barrier prevents CF_2Cl + F formation - clearly the Xe-CF_3Cl* intermediate is not long-lived!

In contrast to this behavior for dissociation, many positive ions have geometries similar to that of the neutral ground state and thus efficient ionization is possible near threshold.

Energetics are also important in dissociation channels leading to 2-atom loss. The above model implies that the first bond cleavage may release considerable energy to translation; only the internal vibronic energy remaining in the molecular fragment is available for its further fragmentation. It is interesting that the data show 2-atom loss to be especially favored, when the resulting fragment could be a (low-energy) double-bonded species. For example, H-atom losses from CH_3OH and C_2H_6 are considerably higher than those from H_2O and CH_4, consistent with formation of CH_2O and C_2H_4 in the former cases. Similarly, C_2H_5OH shows higher H yields than does CH_3OCH_3. A final intriguing example concerns $CF_2Cl \cdot CF_2Cl$ and $CF_3 \cdot CCl_3$: despite having fewer Cl atoms, the former molecule loses significantly more Cl atoms than the latter in the reactions with Kr* and Xe*, suggesting that the stability of $CF_2{=}CF_2$ is the determining factor (clearly $CF_3 \cdot CCl_3$ may respond by losing a F atom with fair efficiency!).

This model, as yet, leaves unexplained a large number of fascinating details. The contrast with photochemistry suggests that the energy transfer and photon excitation populate different subsets of the available Q* vibronic states. The predominance of terminal-bond over central-bond cleavage suggests rather localized bond-excitation by the metastables. To explain these results, speculation is a poor substitute for ab initio calculations, which are beginning to be applied to quenching reactions. The first such calculation on energy transfer from Ar* to H_2 (a relatively slow reaction)[40] lends unexpected support to the model presented here, in showing long range ($\lesssim$ 5 Å) coupling of $Ar^*(^3P) + H_2$ and $Ar + H_2^*(a^3\Sigma_g^+)$, which causes a change in the form of the long-range reactant potential and yields a deep minimum in this potential at shorter range. The surprising strength of the long-range configuration interaction for such a simple system suggests that similar effects may be found in larger molecules. Indirect evidence for these already exists, because attempted correlations of quenching rate constants, using long-range potentials assumed to be dominated by a C_6/R^6 attractive term, fail on a quantitative basis[3] for high-energy excited species, such as the metastable noble gases.

D6. Application to other Excited Species

Because few data exist on the channels for reaction of other electronically-excited species, there is little scope for comparison with our data. The low-lying $O(^1D)$ state is known to induce many atom-transfer channels, e.g.:

$$O(^1D) + RH \rightarrow OH + R \qquad (36)$$

for RH = H_2, H_2O, CH_4, etc. This species thus offers an extreme contrast to the metastable noble gases and other excited species are likely to show intermediate behavior. An example concerns the only other species, Zn, Cd and Hg ($^{1,3}P$), for which an appreciable number of reaction channels have been obtained. These species have lower energies than Xe* and, in agreement with expectation, do not

induce simple dissociation of most H-containing reagents with high efficiency. In fact, the only dominant dissociation channel that has been reported is:[3]

$$Hg^*(^3P) + N_2O \rightarrow Hg + N_2 + O \qquad (37)$$

For other excited species, only total quenching rate constants are available and only predictions, rather than comparisons, of reaction channels are possible. The most general result of our study is that the longest-range interaction dominates the quenching, so that coupling into the continuum of reagent states must compete with other interactions, such as those leading to atom transfer. Our approach would be to examine the set of quenching rate constants for the excited state. Where correlations with absorption thresholds are found, as for the noble gases, it can be suggested that, for the efficient quenchers, dissociation would be the major reaction channel. Examples appear to include the ^3P states of Zn, Cd and Hg[3] (although the interesting reactions with halogen-containing compounds are largely unstudied as yet), $N_2(A^3\Sigma_u^+)$[41] and $N_2(a'^1\Sigma_u^-)$.[42] Where no such correlations are found, the observed quenching rate constants are generally larger than expected and, for these particular cases, quenching channels other than simple dissociation are expected to be important. Examples include the ^1P states of Zn, Cd and Hg,[3] and $CO(a^3\Pi)$,[2] all of which have available atom-transfer channels analogous to those of $O(^1D)$.

Finally, it should be cautioned that the present study was restricted to metastable excited states; additional interactions are possible for resonance excited states, allowing contributions to the quenching also from the long-range dipole-dipole mechanism.

References

1. J. E. Velazco, J. H. Kolts and D. W. Setser, J. Chem. Phys. 69, 4357 (1978).

2. K. Schofield, J. Phys. Chem. Ref. Data. 8, 723 (1979).

3. W. H. Breckenridge, and H. Umemoto, Adv. Chem. Phys. 50, 325 (1982).

4. R. J. Donovan and D. Husain, Chem. Rev. 70, 489 (1970).

5. I. V. Hertel, Adv. Chem. Phys. 50, 475 (1982).

6. T. G. Slanger, Reactions of Electronically Excited Diatomic Molecules, to be published.

7. M. F. Golde, in Gas Kinetics and Energy Transfer, Specialist Periodical Report, 2, 121 (1976).

8. M. F. Golde and R. A. Poletti, Chem. Phys. Lett. 80, 18 (1981).

9. M. F. Golde and R. A. Poletti, Chem. Phys. Lett. 80, 23 (1981).

10. J. Balamuta and M. F. Golde, J. Chem. Phys. 76, 2430 (1982).

11. M. F. Golde, Y-S. Ho and H. Ogura, J. Chem. Phys. 76 3535 (1982).

12. J. Balamuta and M. F. Golde, J. Phys. Chem 86, 2765 (1982).

13. J. Balamuta, M. F. Golde and Y-S Ho, J. Chem. Phys., in press.

14. D. H. Stedman and D. W. Setser, Prog. React. Kin. 6, 193 (1971).

15. K. T. Wu, H. Morgner and A. J. Yencha, Chem. Phys. 68, 285 (1982).

16. C. R. Lishawa, W. Allison, and E. E. Muschlitz, J. Chem. Phys. 77, 5855 (1982).

17. M. S. deVries, V. I. Srdanov, C. P. Hanrahan and R. M. Martin, J. Chem. Phys. 78, 5582 (1983).

18. J. Bel Bruno and J. R. Krenos, J. Chem. Phys. 78, 2800 (1983).

19. R. J. Hennessy and J. P. Simons, Chem. Phys. Lett. 75, 43 (1980).

20. M. Tsuji, I. Murakami and Y. Nishimura, J. Chem. Phys. 75, 5373 (1981).

21. M. Suto and N. Washida, J. Chem. Phys. 78, 1007 (1983).

22. L. A. Gundel, D. W. Setser, M. A. A. Clyne, J. A. Coxon and W. Nip, J. Chem. Phys. 64, 4390 (1976).

23. J. H. Kolts, J. E. Velazco and D. W. Setser, J. Chem. Phys. 71, 1247 (1979).

24. J. E. Velazco, J. H. Kolts and D. W. Setser, J. Chem. Phys. 65, 3468 (1976).

25. K. Tamagake, D. W. Setser and J. H. Kolts, J. Chem. Phys. 74, 4286 (1981).

26. A. S. Werner, B. P. Tsai and T. Baer, J. Chem. Phys. 60, 3650 (1974).

27. R. M. Martin and T. P. Parr, J. Chem. Phys. 70, 2220 (1979).

28. D. L. Dexter, J. Chem. Phys. 21, 836 (1953).

29. D. R. Herschbach, Adv. Chem. Phys. 10, 319 (1966).

30. W. Goy, V. Kohls and H. Morgner, J. Electron Spectrosc. 23, 383 (1981).

31. W. Goy, H. Morgner and A. J. Yencha, J. Electron Spectrosc. 24, 77 (1981).

32. P. Botschwina, W. Meyer, I. V. Hertel, and W. Reiland, J. Chem. Phys. 75, 5438 (1981).

33. H. Okabe, Photochemistry of Small Molecules, Wiley, (1978).

34. A. H. Laufer and J. R. McNesby, J. Chem. Phys. 49, 2272 (1968).

35. S. G. Lias, G. J. Collin, R. E. Rebbert and P. Ausloos, J. Chem. Phys., 52, 1841 (1970).

36. R. L. Lilly, R. E. Rebbert and P. Ausloos, J. Photochem. 2, 49 (1973/74).

37. W. E. Groth, H. Okabe and H. J. Rommel, Z. Naturforsch. Teil A 19, 507 (1964).

38. S. Glicker and L. J. Stief, J. Chem. Phys. 54, 2852 (1971).

39. M. S. Gordon and J. W. Caldwell, J. Chem. Phys. 70, 5503 (1979).

40. R. P. Blickensderfer, K. K. Sunil and K. D. Jordan, J. Phys. Chem. 87, 1488 (1983).

41. W. G. Clark and D. W. Setser, J. Phys. Chem. 84, 2225 (1980).

42. M. F. Golde, unpublished results.

TABLE 1.

Properties of the lowest metastable excited states of the noble gas atoms.

Atom	State	Energy cm^{-1}	Energy eV.	Radiative Lifetime, sec
He	$1s2s\ ^1S$	166272	20.6	~0.02
	^3S	159850	19.8	~9000
Ne	$2p^53s\ ^3P_0$	134821	16.7	430
	$^3P_2$	134044	16.6	>0.8
Ar	$3p^54s\ ^3P_0$	94554	11.7	45
	$^3P_2$	93144	11.5	>1.3
Kr	$4p^55s\ ^3P_0$	85192	10.5	0.5
	$^3P_2$	79973	9.9	>1.0
Xe	$5p^56s\ ^3P_0$	76197	9.4	0.08
	$^3P_2$	67068	8.3	~150

TABLE 2

Total Quenching Rate Constants[a] ($10^{-11}cm^3s^{-1}$) for $Ar(^3P_2)$, $Kr(^3P_2)$ and $Xe(^3P_2)$

Reagent	$Ar(^3P_2)$	$Kr(^3P_2)$	$Xe(^3P_2)$
H_2	6.6	3.0	1.6
CO	1.4	5.8	3.6
N_2	3.6	0.39	1.9
NO	22	19	27
N_2O	44	31	44
O_2	21	16	22
SO_2	64	58	
CO_2	53	40	45
OCS	79		
HCl	37		56
HBr	52		61
Cl_2	71	73	72
Br_2	65	61	60
SF_6	16	18	23
CF_3Br	31	50	42
PCl_3	53		46
CF_3Cl	22	14	10
CF_2Cl_2	37		19
$CFCl_3$	55		33
CCl_4	100	69	63

a. Ref. 1

TABLE 2 (continued)

Total Quenching Rate Constants ($10^{-11}cm^3s^{-1}$) for $Ar(^3P_2)$, $Kr(^3P_2)$ and $Xe(^3P_2)$

Reagent	$Ar(^3P_2)$	$Kr(^3P_2)$	$Xe(^3P_2)$
CH_3Cl	75		
CH_2Cl_2	85		
$CHCl_3$	105		
CF_4	4	0.07	0.03
CF_3H	31	15	0.2
CH_4	33	37	33
H_2O	48		
CH_3OH	60		
NH_3	54	90	
C_2H_6	66	50	64

TABLE 3

Saturation ion-currents and atom yields (relative to 2.0 for O_2, Cl_2 and H_2) in the reactions of Ar* in the absence and presence of SF_6.

Ar flow rate: 3×10^{-4} mol s^{-1}, total pressure: 1.0-1.2 Torr, $[SF_6] = (3\text{-}6) \times 10^{12}$ cm^{-3}.

Reagent	Ionization Potential, eV	Saturation Ion current, μA		Atom	Atom Yields	
		No SF_6[a]	SF_6 present		No SF_6	SF_6 present
NH_3	10.2	3.8	7.40	H	0.91 ± 0.05	0.62 ± 0.04
CH_2O	10.9	4.6	6.56	H	0.90 ± 0.06	0.80 ± 0.04
				O	0.18 ± 0.04	0.21 ± 0.03
CH_3OH	10.8	1.7	3.97	H	1.64 ± 0.08	1.45 ± 0.03
				O	0.06 ± 0.02	0.05 ± 0.03
C_2H_5OH	10.5	1.5	3.16	H	1.58 ± 0.08	1.34 ± 0.06
CH_3OCH_3	10.0	2.5	4.40	H	1.22 ± 0.04	1.06 ± 0.04
OCS	11.2	6.0	9.4	O	0.10 ± 0.02	0.06 ± 0.02
CH_3Cl	11.3	~4.1	8.1	H	0.58 ± 0.05	0.39 ± 0.03
				Cl	0.38 ± 0.03	0.26 ± 0.02
CH_2Cl_2	11.3	3.6	5.20	H	0.36 ± 0.02	0.36 ± 0.02
				Cl	1.21 ± 0.04	0.95 ± 0.04
CH_3Br	10.5	5.3	8.1		-	-

a: Applied voltage at ion-collection electrodes: 150V.

TABLE 4

Branching Fractions for Chemiionization Reactions of Ar*

Reagent	Ionization Potential, eV	Branching Fraction
NO	9.25	0.28
OCS	11.17	0.47
NO_2	9.79	<0.001
Cl_2	11.48	0.02
Br_2	10.54	0.04
HBr	11.62	0.12
PCl_3	9.91	0.22
CCl_4	11.47	0.12
$CHCl_3$	11.42	0.15
CH_2Cl_2	11.35	0.26
CH_3Cl	11.3	0.42
$CHBr_3$	10.51	0.39
CH_2Br_2	10.49	0.57
CH_3Br	10.53	0.41
CH_2I_2	~ 9.6	~ 0.4
CH_3I	9.54	0.41
$CFBr_3$	~ 10.9	0.32
CF_2Br_2	~ 11.4	0.33
CF_3Br	11.89	0.03
NH_3	10.2	0.42 ± 0.04
CH_2O	10.9	0.33
CH_3OH	10.8	0.20 ± 0.01
C_2H_5OH	10.5	0.16 ± 0.01
CH_3OCH_3	10.0	0.21 ± 0.01
C_2H_6	11.5	0.01

TABLE 5

Branching fractions for ionization by $Ar(^3P_0)$ and $Ar(^3P_2)$.

Reagent	Ionization Potential, eV	α_0[b]	f_2	f_0[c]
CCl_4	11.3–12[a]	0.15	0.11	0.25 ± 0.02
$CHCl_3$	11.4–12[a]	0.10	0.14	0.21 ± 0.02
CH_2Cl_2	11.3–11.8[a]	0.10	0.25	0.37 ± 0.03
CH_3Cl	11.3–11.6[a]	0.070	0.42	0.42 ± 0.03
CBr_4	10.31	0.052	0.26	0.19 ± 0.02
$CHBr_3$	10.48	0.070	0.40	0.40 ± 0.03
CH_2Br_2	10.52	0.080	0.58	0.67 ± 0.05
CH_3Br	10.54	0.056	0.42	0.33 ± 0.03
$CFBr_3$	~ 10.9	0.071	0.32	0.32 ± 0.03
CF_2Br_2	~ 11.4	0.091	0.32	0.43 ± 0.03
CF_3Br	11.89	0.30	0.02	0.11 ± 0.01
HBr	11.67	0.49	0.05	0.62 ± 0.03
DBr	11.67	0.48	0.05	0.69 ± 0.03
NH_3	10.2	0.091	0.35	0.49 ± 0.04
CH_3OH	10.8	0.059	0.20	0.16 ± 0.02

a. First entry: adiabatic ionization potential; range is that of first strong band in photoionization spectrum.

b. $\alpha_0 = f_0[^3P_0]/(f_0[^3P_0]+f_2[^3P_2])$

c. $[^3P_0]/([^3P_0]+[^3P_2]) = 0.070 \pm 0.005$

TABLE 6

Saturation ion currents and relative branching fractions for Chemiionization Reactions of Ne*.

Reagent	Ionization Potential, eV	Saturation Ion Current, μA[a]	Relative Branching Fraction[a]
Ar	15.8	0.36	1.0
Kr	14.0	0.22	0.67
N_2	15.6	0.28	0.78
H_2	15.4	0.22	0.59
CO	14.0	0.24	0.68
O_2	12.1	0.21	0.55
N_2O	12.9	0.25	0.69
CO_2	13.8	0.26	0.68
NO	9.2	0.24	0.74
Cl_2	11.5	0.093	0.30
H_2O	12.6	0.15	0.54
NO_2	9.8	0.10	0.28
DBr	11.6	0.28	0.75
CH_4	12.6	0.24	0.72
CH_3Cl	10.3	0.38	1.0
CH_2Br_2	10.5	0.29	0.76
CF_4	13.4	0.15	0.45
$CFBr_3$	10.9	0.27	0.72

a. Ne* + Ar was used as the reference reaction in each experiment to allow conversion of ion currents to relative branching fractions.

TABLE 7

Emission Channels in the Reactions of Ar*.

Reagent	Emitting States	Branching fraction	Ref.
H_2	$H_2(a^3\Sigma_g^+)$	0.05	a
N_2	$N_2(C^3\Pi_u)$	0.8 ± 0.2	a
N_2O	$N_2(B^3\Pi_g)$	0.96	22
	$NO(B^2\Pi)$	0.03	22
CO_2	$CO(a^3\Pi)$	0.16 ± 0.08	a
SO_2	$SO(A^3\Pi, B^3\Sigma^-)$	0.03 ± 0.01	a
OCS	CO*, S*	0.04	22
H_2O	$OH(A^2\Sigma^+)$	0.28 ± 0.09	a
NO_2	$NO(A^2\Sigma^+, B^2\Pi, D^2\Sigma^+, B'^2\Delta)$	0.13	a
CH_2O	$CO(a^3\Pi)$	~ 0.08	a
HCl	$ArCl(B(1/2))$, $HCl(V^1\Sigma^+)$	0.03	22
Cl_2	$ArCl^*, Cl_2^*, Cl(4^2, {}^4P_J)$	1.00	22
Br_2	$Br(5^2, {}^4P_J)$	1.00	22
CF_3Br	$Br(5^2, {}^4P_J)$	0.03	a
CF_2Br_2	$Br(5^2, {}^4P_J)$	0.13	a
$CFBr_3$	$Br(5^2, {}^4P_J)$	0.21	a
CBr_4	$Br(5^2, {}^4P_J)$	0.21	a
CCl_4	ArCl(B,C)	0.06	22
Xe^*+CCl_4	XeCl(B,C)	0.13	23
$Xe^*+ CFCl_3$	XeCl(B,C)	0.15	23

a: This work

TABLE 8

Relative Formation Rates of $Br^{*2,4}P_J$ by Reaction of $Ar^{*3}P_{0,2}$.

(a) Ar^3P_2 +	CF_3Br	CF_2Br_2	$CFBr_3$	CBr_4	Br_2[b]	$CHBr_3$	PBr_3[b]
$Br^{*2}P_{1/2}(68964)$[a]	c	0.005	0.024	0.097	0.103	0.014	0.027
$^2P_{3/2}(67177)$	0.055	0.21	0.187	0.189	0.210	0.182	0.164
$^4P_{1/2}(66877)$	0.010	0.012	0.040	0.119	0.118	0.032	0.052
$^4P_{3/2}(64900)$	1	1	1	1	1	1	1
$^4P_{5/2}(63430)$	1.45	0.67	0.63	0.57	(0.72)	0.91	0.83
(b) Ar^3P_0 reaction.							
$Br^{*2}P_{1/2}$	~0.04	0.16	0.16	0.16	0.11	0.17	0.14
$^2P_{3/2}$	0.24	0.23	0.22	0.30	0.34	0.23	0.33
$^4P_{1/2}$	0.17	0.58	0.51	0.51	0.24	0.61	0.72
$^4P_{3/2}$	1	1	1	1	1	1	1
$^4P_{5/2}$	2.2	0.77	0.63	0.60	d	0.62	0.75

a. Energy in cm^{-1}. b. Calculated from distribution in absence of Kr or CO.
c. Endothermic channel. d. Masked by $Kr^* + Br_2$ reaction.

Table 9

Branching fractions for total Br* emission from reactions of $Ar(^3P_0)$ and $Ar(^3P_2)$.

Reagent	α_0	f_2	f_0[a]
Br_2	0.10	1.0	1.0
CF_3Br	0.042	0.03	0.013
CF_2Br_2	0.037	0.14	0.048
$CFBr_3$	0.081	0.21	0.17
CBr_4	0.104	0.21	0.22
CH_2Br_2	0.012	0.034	0.004
$CHBr_3$	0.084	0.12	0.10

a. $[^3P_0]/([^3P_0] + [^3P_2]) = 0.10$

Table 10

Relative oxygen atom yields

Reagent	Ar*	Kr*	Xe*
O_2	2	2	2
CO_2	0.98(2)[a]	1.02(8)	0.98(2)
SO_2	0.94(4)	0.96(6)[b]	1.00(2)
N_2O	1.12(2)	1.04(6)	0.82(4)
CO	0.84(2)	0±0.02	0±0.02
OCS	0.06(2)	0.12(2)	0.06(2)
NO	>1.38(6)[c]	>1.34(4)[c]	>1.66(4)[c]
NO_2	>0.98(6)[d]	-	-

a. 0.98 ± 0.02

b. At low $[SO_2]$. The O-signal decreases to 0.80 ± 0.06 at high $[SO_2]$.

c. Lower limits, as the secondary reaction, $N + NO \rightarrow N_2 + O$, may not have been driven to completion.

d. Lower limit, as removal of O by $O + NO_2 \rightarrow NO + O_2$ is occurring.

TABLE 11

Yields of oxygen and hydrogen atoms (relative to 2.00 for reactions with O_2 and H_2)

Reagent	Atom	Atom yields (Ar*)	(Kr*)	(Xe*)
H_2O	H	1.52 ± 0.10	1.08 ± 0.06	1.00 ± 0.06
	O	0.46 ± 0.04	0.14 ± 0.04	0 ± 0.02
D_2O	D	1.42 ± 0.06	1.08 ± 0.08	1.00 ± 0.14
	O	0.48 ± 0.02	0.10 ± 0.02	0 ± 0.02
NH_3	H	0.62 ± 0.04	1.10 ± 0.05	1.04 ± 0.06
CH_4	H	1.53 ± 0.08	1.10 ± 0.04	0.98 ± 0.02
CH_2O	H	0.80 ± 0.04	1.68 ± 0.08	1.90 ± 0.08
	O	0.21 ± 0.03	0.09 ± 0.02	0.03 ± 0.01
CH_3OH	H	1.45 ± 0.03	1.70 ± 0.04	1.49 ± 0.03
	O	0.05 ± 0.03	0 ± 0.02	0 ± 0.02
CH_3OD	H	1.01 ± 0.03	1.12 ± 0.04	0.81 ± 0.02
	D	0.46 ± 0.04	n.m.[a]	0.68 ± 0.02
C_2H_5OH	H	1.34 ± 0.06	1.42 ± 0.06	1.22 ± 0.06
	O	0 ± 0.02	0 ± 0.02	0 ± 0.02
C_2H_5OD	H	0.94 ± 0.06	0.98 ± 0.04	0.72 ± 0.04
	D	0.32 ± 0.02	n.m.	0.52 ± 0.02
CH_3OCH_3	H	1.06 ± 0.04	n.m.	0.86 ± 0.04
	O	0 ± 0.02	n.m.	0 ± 0.02
C_2H_6	H	1.82 ± 0.04	1.68 ± 0.08	1.08 ± 0.04
CF_3H	H	0.75 ± 0.03	0.75 ± 0.04	0.89 ± 0.04

a: n.m. - not measured.

TABLE 12

Yields of chlorine and hydrogen atoms (relative to 2.00 for reactions with Cl_2 and H_2)

Reagent	Atom	Atom yields (Ar*)	(Kr*)	(Xe*)
HCl	H	1.00(5)[a]	1.01(6)	0.99(3)
	Cl	0.96(5)	1.00(3)	1.00(3)
CF_3Cl	Cl	0.95(3)	0.97(2)	0.97(2)
CF_2Cl_2	Cl	1.64(6)	1.50(6)	1.96(8)
$CFCl_3$	Cl	2.16(12)	1.68(4)	1.80(6)
CH_3Cl	H	0.39(3)	0.63(4)	0.57(4)
	Cl	0.26(2)	0.31(2)	0.27(1)
CH_2Cl_2	H	0.36(2)	0.33(5)	0.28(3)
	Cl	0.95(4)	1.04(3)	0.76(3)
$CHCl_3$	H	0.25(2)	0.23(4)	0.25(3)
	Cl	1.41(4)	1.25(3)	0.99(4)
CCl_4	Cl	1.97(8)	1.50(5)	1.32(4)
CF_2HCl	H	0.73(6)	n.m.	0.36(5)
	Cl	0.90(5)	0.83(4)	0.85(4)
$CFHCl_2$	H	0.40(5)	n.m.	0.21(5)
	Cl	1.41(6)	1.03(4)	0.93(4)
$CF_2Cl \cdot CF_2Cl$	Cl	1.36(5)	1.23(4)	1.72(5)
$CF_3 \cdot CCl_3$	Cl	1.48(6)	1.19(5)	1.38(5)

a: 1.00 ± 0.05.

TABLE 13

Energetics and Branching Fractions for Dissociation channels.

Reagent	Products	Threshold energy,eV	Branching fractions Ar*	Kr*	Xe*
H_2O	O + H + H	9.5	0.46 ± 0.05	0.11 ± 0.05	—a
	OH + H	5.1	0.54 ± 0.04	0.86 ± 0.04	1.00 ± 0.06
	O + H_2	5.0	0	0.03 ± 0.03	0 ± 0.06
NH_3	NH + 2H	8.5			—a
	N + H_2 + H	7.6			1.00 ± 0.06
	NH_2 + H	4.6			
	NH + H_2	4.0			0 ± 0.06
CH_4	CH_2 + 2H	9.3	0.65 ± 0.12		—a
	CH + H_2 + H	9.2			—a
	CH_3 + H	4.5	0.35 ± 0.12		0.98 ± 0.02
	CH_2 + H_2	4.8			0.02 ± 0.02
CH_2O	CH_2 + O	7.7	0.21 ± 0.03[b]	0.09 ± 0.02	0.03 ± 0.01
	CO + 2H	4.5	0.37 ± 0.05[b]	0.81 ± 0.07	0.94 ± 0.04
	CHO + H	3.8	0.06 ± 0.07[b]	0.07 ± 0.10	< 0.04 ± 0.04
	CH + OH	7.7	0.03 ± 0.05[b]	0.03 ± 0.06	< 0.02 ± 0.04
	CO + H_2	0.0			

TABLE 13 (continued)

Energetics and Branching Fractions for Dissociation channels.

Reagent	Products	Threshold energy, eV	Branching fractions Ar*	Kr*	Xe*
CH_3OH	$CH_3 + O + H$	8.4			0 ± 0.02
	$CH_2O + 2H$	5.4			0.58 ± 0.10
	$CH_3O + H$	4.5			0.10 ± 0.10
	$CH_2OH + H$	4.0			0.22 ± 0.11
	$CH_3 + OH$	4.0			0.10 ± 0.11
C_2H_6	$C_2H_4 + 2H$	5.9	0.86 ± 0.05[c]	0.76 ± 0.08	
	$C_2H_5 + H$	4.2	0.09 ± 0.09[c]	0.16 ± 0.16	
	$CH_3 + CH_3$	3.9	0.04 ± 0.04[c]	0.08 ± 0.08	
	$C_2H_4 + H_2$	1.4			
CF_3Cl	$CF_2 + ClF$	6.3	< 0.05	< 0.03	< 0.03
	$CF_2Cl + F$	5.4	< 0.05	< 0.03	< 0.03
	$CF_2 + F + Cl$	9.0	0.95 ± 0.03	0.97 ± 0.02	—a
	$CF_3 + Cl$	3.7			0.97 ± 0.02

TABLE 13 (continued)

Energetics and Branching Fractions for Dissociation channels.

Reagent	Products	Threshold energy, eV	Branching fractions Ar*	Kr*	Xe*
CF_2Cl_2	ACl^* + CF_2Cl				< 0.03
	CFCl + F + Cl	9.0	0.25 ± 0.25		--a
	CF + Cl + ClF	8.5			--a
	CCl_2 + F_2	7.6			< 0.02 ± 0.06
	CFCl + ClF	6.3			
	CF_2 + 2Cl	5.7		0.62 ± 0.13	0.94 ± 0.06
	$CFCl_2$ + F	4.9			< 0.02 ± 0.06
	CF_2Cl + Cl	3.6			< 0.04 ± 0.06
	CF_2 + Cl_2	3.2			< 0.02 ± 0.06
$CFCl_3$	ACl^* + $CFCl_2$				0.15
	CFCl + 2Cl	5.8			0.81 ± 0.06
	CF + Cl + Cl_2	6.9			< 0.04 ± 0.06
	$CFCl_2$ + Cl	3.2			
	CCl_2 + ClF	6.3			< 0.02 ± 0.06
	CCl_3 + F	4.6			
	CFCl + Cl_2	3.3			

TABLE 13 (continued)

Energetics and Branching Fractions for Dissociation channels.

Reagent	Products	Threshold energy, eV	Branching fractions Ar*	Kr*	Xe*
CCl_4	$AC1^*$ + CCl_3		0.06	~0.10	0.13
	CCl + 3Cl	10.0	> 0.15[d]	--a	--a
	CCl_2 + 2Cl	6.0		0.60 ± 0.10	0.46 ± 0.14
	CCl + Cl + Cl_2	7.5		0.20 ± 0.20	0.28 ± 0.28
	CCl_3 + Cl	3.0			
	CCl_2 + Cl_2	3.0		0.10 ± 0.10	0.13 ± 0.13
CH_3Cl	CH_2Cl + H	4.4			0.57 ± 0.04
	CHCl + H_2	4.0			0.16 ± 0.05[e]
	CH_2 + HCl	3.9			
	CH_3 + Cl	3.6			0.27 ± 0.01

a: endothermic channels
b: the uncertainties do not take account of the uncertainties in f_{ion}.
c: assuming that dissociation to C_2H_3 + 3H is unimportant.
d: The first direct evidence for 3-atom elimination.
e: The first evidence for molecular elimination.

Figure Captions

Figure 1 Experimental reaction vessel for resonance fluorescence measurements. A: Movable reagent loop; B, C: Reagent inlets; W: MgF_2 window; M: Microwave cavity.

Figure 2 Reaction vessel for saturation ion-current measurements.

Figure 3 Dependence of ion current on applied electrode potential.

Triangles: no SF_6. (Δ)Ar* + C_2H_5OH,
(▲) Ar* + CH_3OCH_3. Circles: SF_6 present.
(○) Ar* + C_2H_5OH, $[SF_6] = 8 \times 10^{12}$ cm^{-3};
(●) Ar* + CH_3OCH_3, $[SF_6] = 2 \times 10^{12}$ cm^{-3}.

Figure 4 Dependence of saturation ion current, I, on concentration of Kr added upstream of reagent inlet.
I_o: ion current in the absence of Kr.
(+) Ar* + HBr; (□) Ar* + CF_3Br;
(○) Ar* + CH_3Br.

Figure 5 Vacuum UV emission spectra of (a) $Ar(^3P_0)$ + CCl_4 and (b) $Ar(^3P_2)$ + CCl_4. Dashed line: spectral response function.

Figure 6 The dependence of emission intensities at 121.6 nm on $[H_2]$ in the reaction of Xe* with H_2. (●) Background emission; (■) scattered light from the resonance lamp; (I) the resonance fluorescence signal.

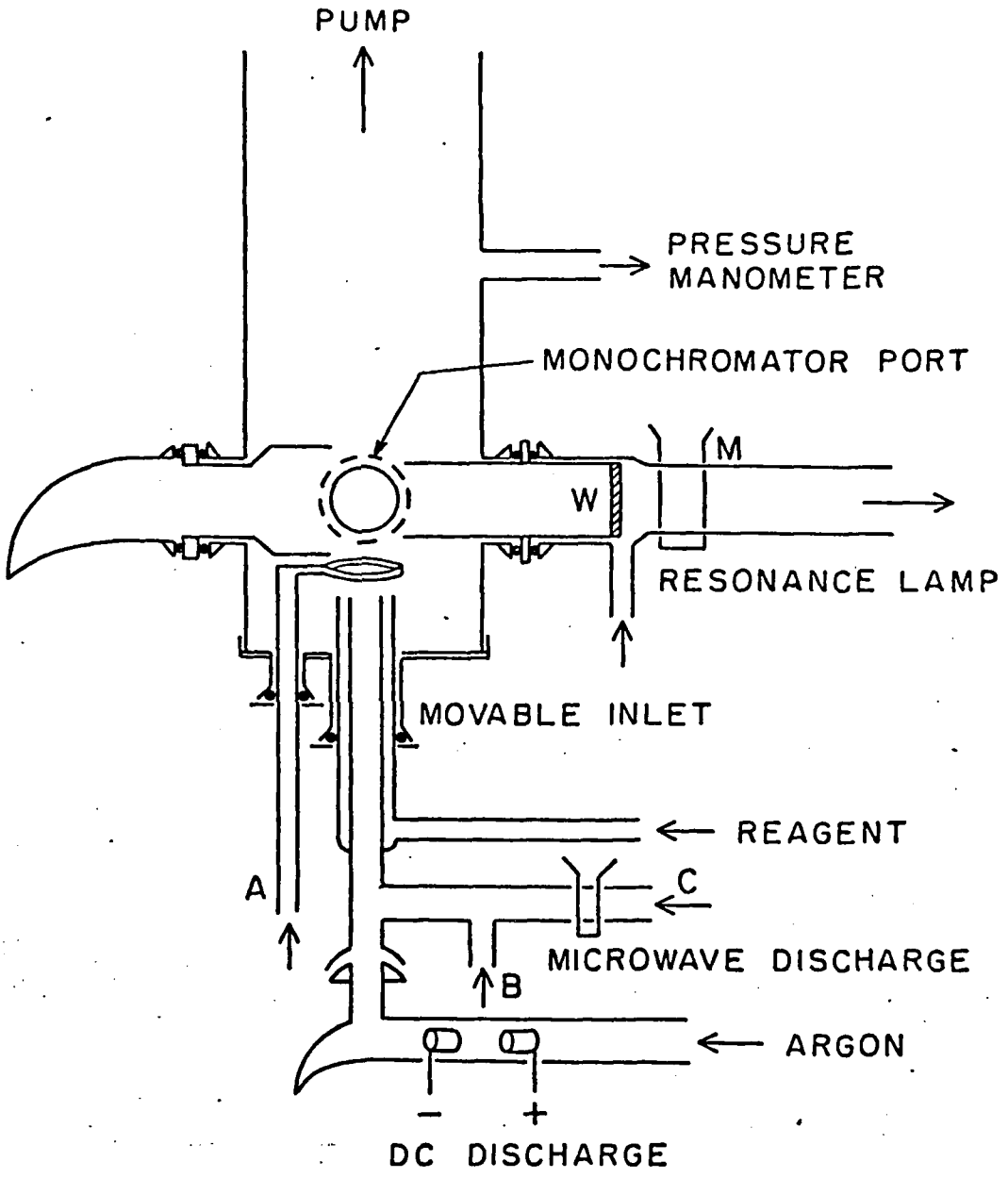
PUMP
PRESSURE
MANOMETER
MONOCHROMATOR PORT
M
W
RESONANCE LAMP
MOVABLE INLET
REAGENT
A
C
MICROWAVE DISCHARGE
B
ARGON
−
+
DC DISCHARGE

FIG. 1.

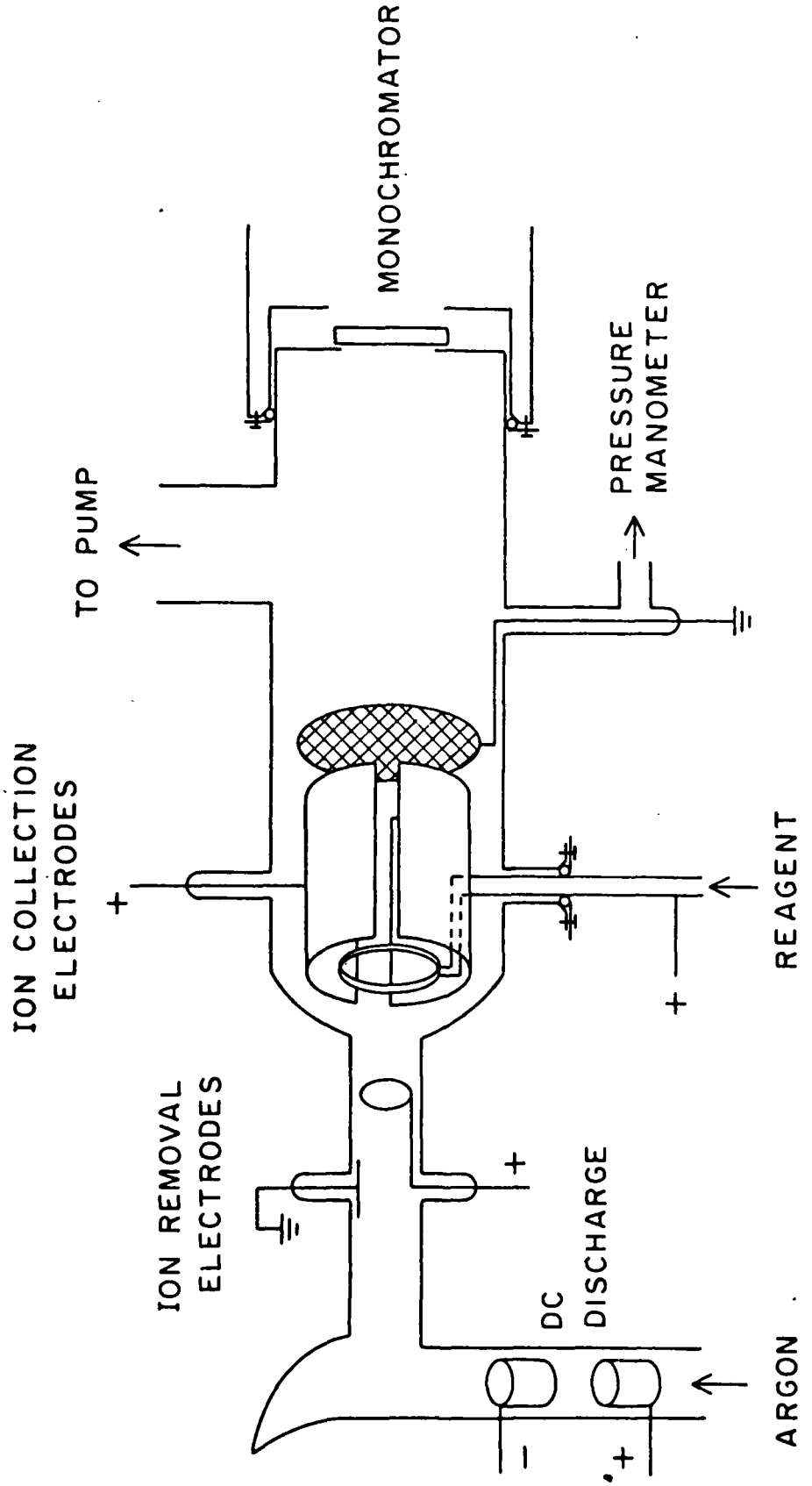

FIG. 2. REACTION VESSEL FOR SATURATION ION CURRENT MEASUREMENTS

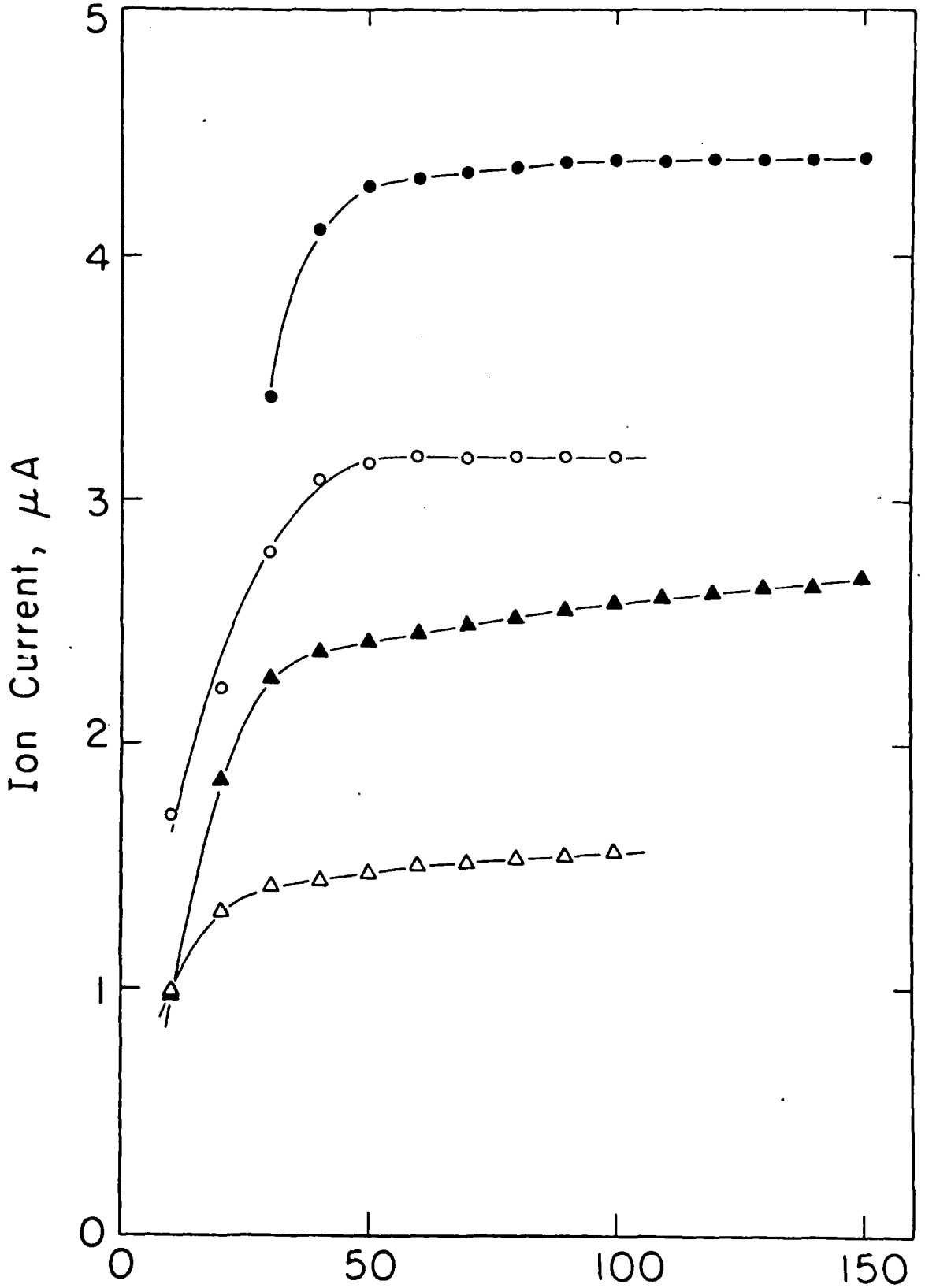

Fig. 3.

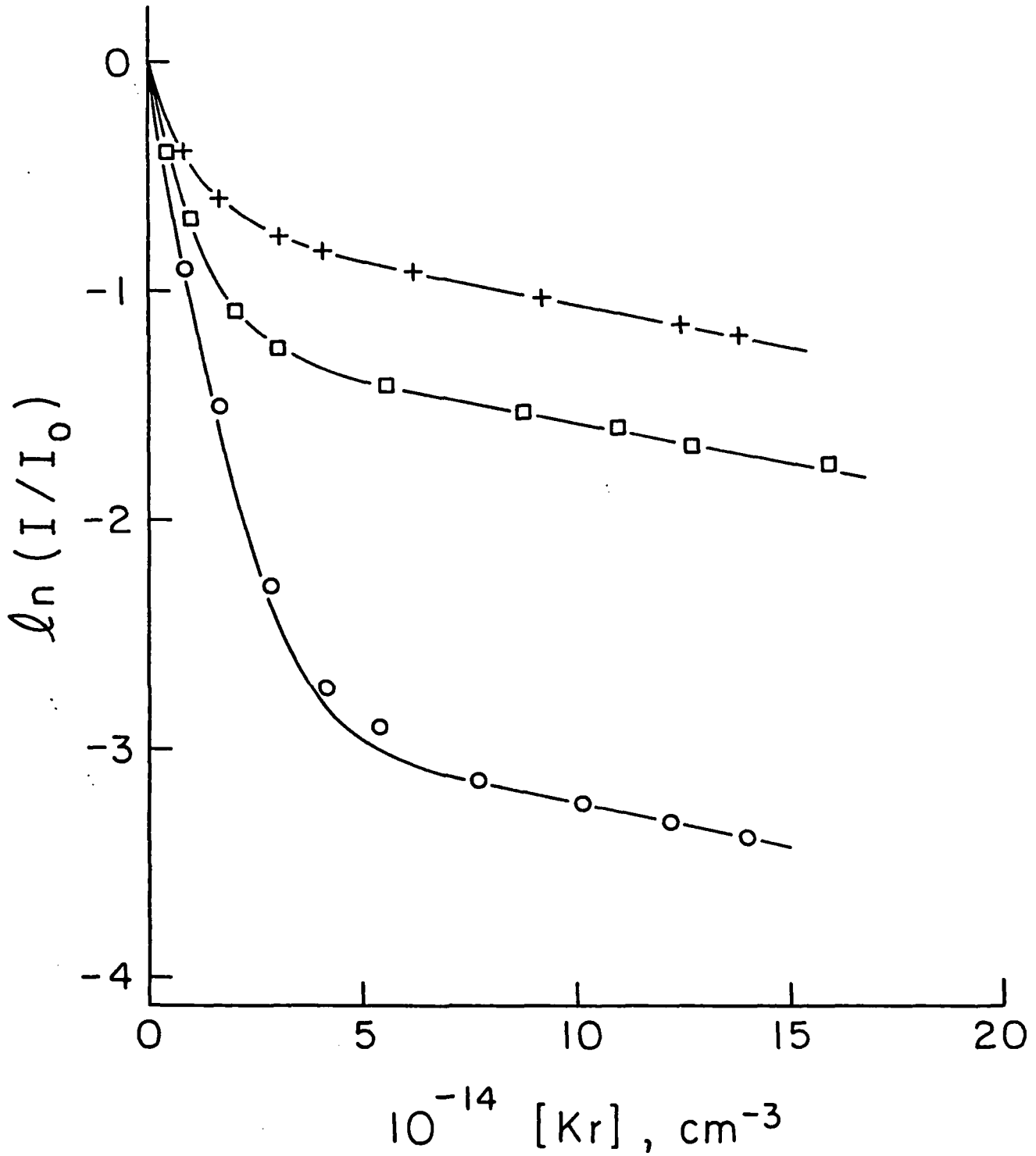

FIG. 4.

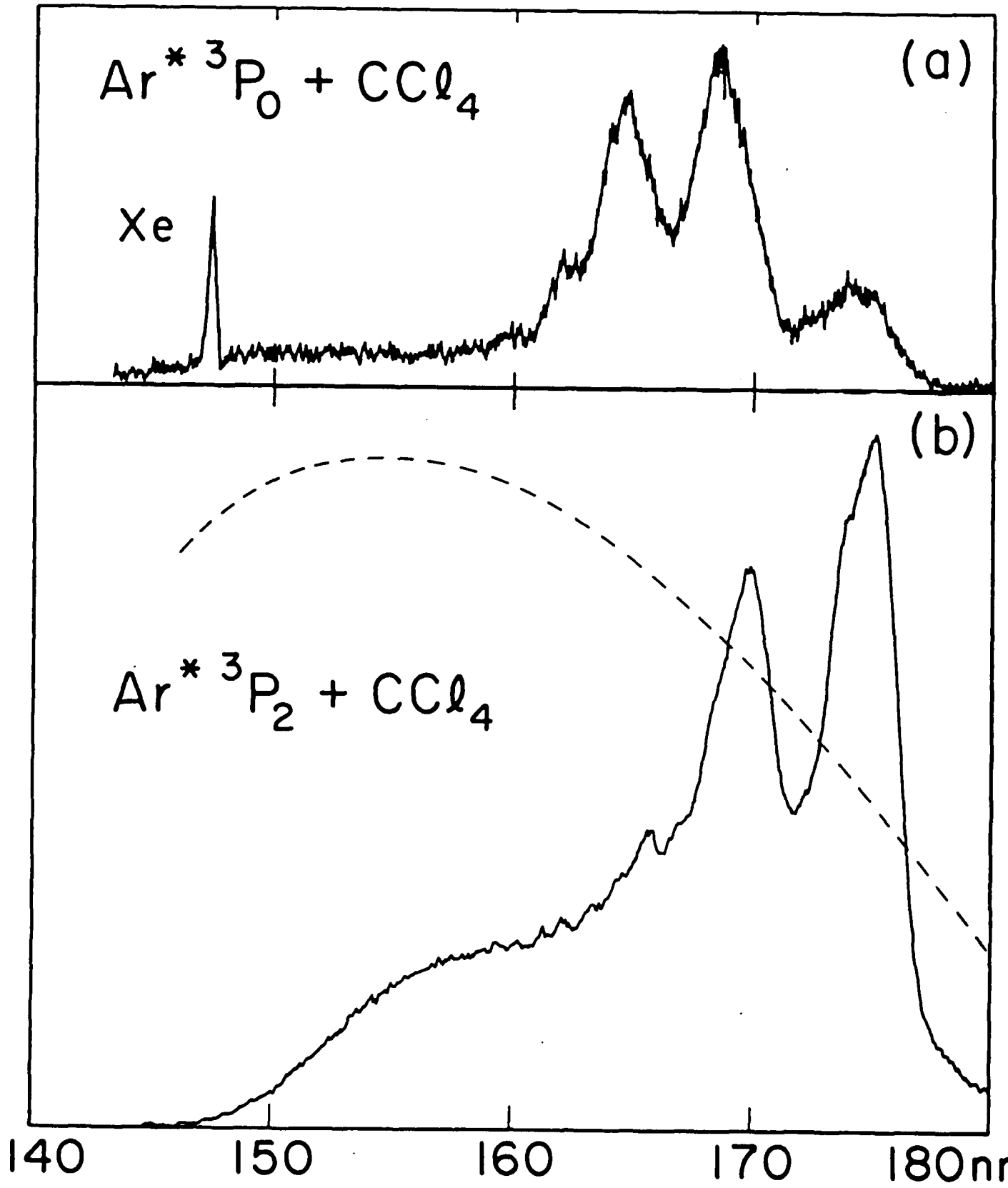

FIG 5.

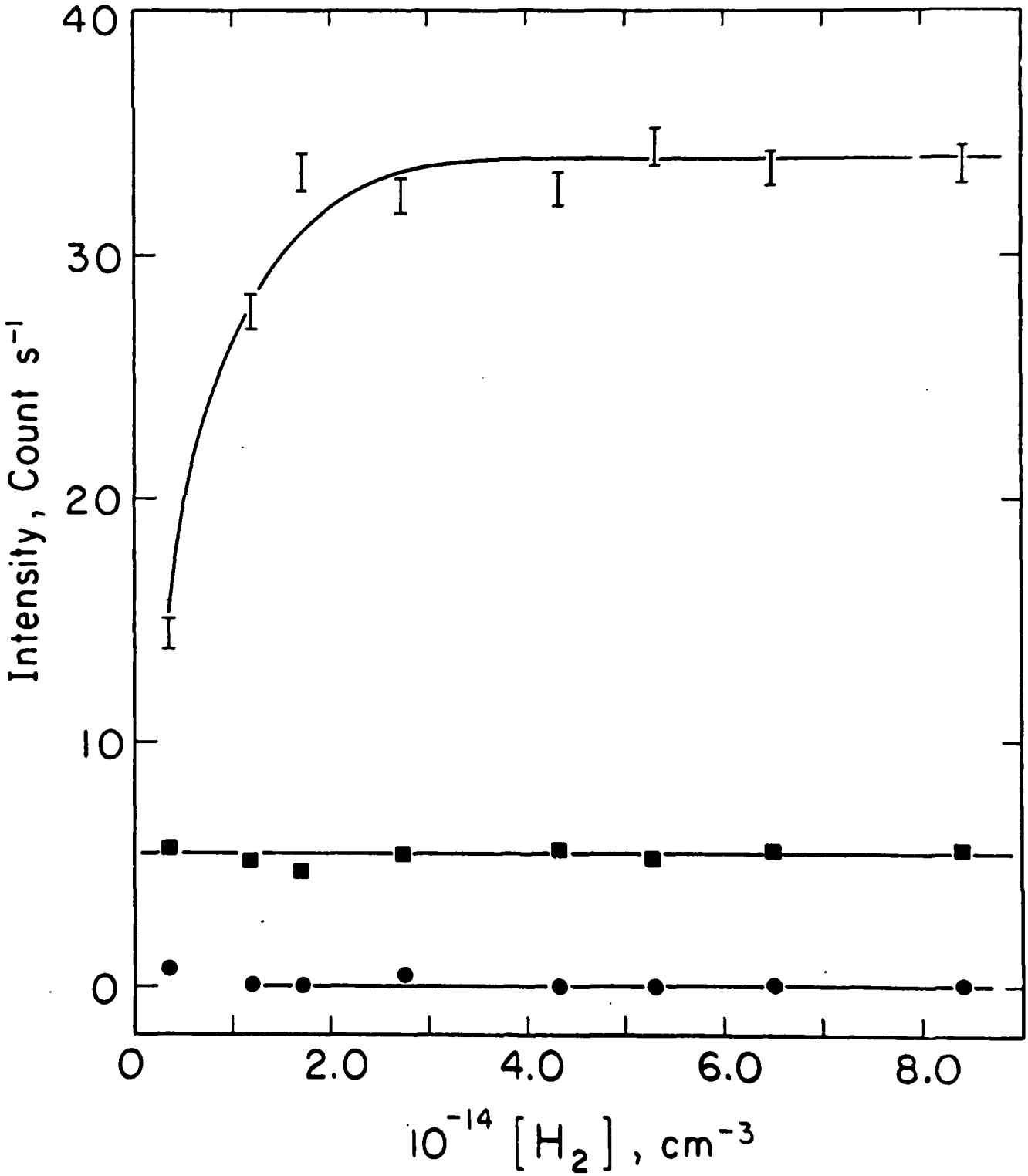

FIG. 6.

Publications

1,2. M. F. Golde and R. A. Poletti, Comparison of Reactivity of $Ar(^3P_0)$ and $Ar(^3P_2)$ Metastable Species.
I. Rate Constants for Quenching by Kr and CO.
II. Products of Quenching by some Halogen-Containing Compounds.
Chem. Phys. Lett. 80, 18, 23 (1981).

3. J. Balamuta and M. F. Golde. Quenching of metastable Ar, Kr, and Xe atoms by oxygen-containing compounds: a resonance fluorescence study of reaction products. J. Chem. Phys. 76, 2430 (1982).

4. M. F. Golde, Y-S. Ho and H. Ogura. Chemiionization reactions of metastable $Ar(^3P_{0,2})$ atoms. J. Chem. Phys. 76, 3535 (1982).

5. J. Balamuta and M. F. Golde. Formation of electronically-excited oxygen atoms in the reactions of $Ar(^3P_{0,2})$ and $Xe(^3P_2)$ atoms with O_2. J. Phys. Chem., 86, 2765 (1982).

6. J. Balamuta, M. F. Golde, and Y-S. Ho. Product distributions in the reactions of excited noble-gas atoms with hydrogen-containing compounds, J. Chem. Phys., in press.

In Preparation (J. Chem. Phys.)

M. F. Golde and A. M. Moyle, XeBr excimer formation in the reactions of $Xe(^3P_2)$ excited atoms with HBr and DBr.

M. F. Golde, Y-S. Ho and H. Ogura, Chemiionization in reactions of state-selected $Ar(^3P_2)$ and $Ar(^3P_0)$ excited atoms with small molecules.

J. Balamuta, M. F. Golde, and A. M. Moyle, Product distributions in the reactions of excited noble-gas atoms with chlorine-containing compounds.

Personnel

John Balamuta:	Graduate Research Student, May 1979 to April 1983. Degree: Ph.D. Thesis Title: Spectroscopic studies of energy transfer from metastable noble gas atoms.
Yueh-Se Ho:	Graduate Research Student, Sept. 1980 to present.
Alfred M. Moyle:	Graduate Research Student, Jan. 1982 to present.
Hiroo Ogura:	Postdoctoral Research Associate, June 1980 to May 1982.

Invited Seminars, etc.

May 1981 Harvard University
Physical Sciences Inc.

May 1982 University of Utah
University of Colorado, Boulder
Kansas State University.

END

FILMED

3-84

DTIC